Supporting Information (*SI*)

Optical Control of Cardiac Function with a Photoswitchable Muscarinic Agonist

Fabio Riefolo¶, Carlo Matera¶, Aida Garrido-Charles, Alexandre M. J. Gomila, Rosalba Sortino, Luca Agnetta, Enrique Claro, Roser Masgrau, Ulrike Holzgrabe, Montserrat Batlle, Michael Decker, Eduard Guasch, and Pau Gorostiza*

Contents

1. Chemical synthesis

1.1 Materials and methods

All reagents and solvents were purchased from Sigma-Aldrich and Serviquimia and were used without any further purification. All reactions were performed under inert atmosphere of argon or nitrogen, unless differently stated**.** TLC analyses were performed on commercial silica gel 60 F_{254} aluminium foils (Merck); spots were further evidenced by spraying with a dilute alkaline potassium permanganate solution or a phosphomolybdic acid solution 5% in ethanol and, for tertiary amines and quaternary ammonium compounds, with the Dragendorff reagent. Flash chromatography was performed on PanReac AppliChem silica gel 60 (40-63 microns) as stationary phase; mobile phases are specified for each compound. UV/Vis spectra and experiments were recorded with a Shimadzu UV-1800 UV-VIS Spectrophotometer with standard quartz cuvettes (10 mm light path).

^{1}H-NMR, ^{13}C-NMR, COSY and HSQC spectra were registered with a Varian Mercury 400 MHz instrument (400 MHz for ^{1}H-NMR and 101 MHz for ^{13}C-NMR) in DMSO-d_6, $CDCl_3$, CD_3OD. Residual signals of the deuterated solvents were used as an internal standard (DMSO-*d*6: ^{1}H 2.50 *ppm*, ^{13}C 39.52 *ppm*; $CDCl_3$: ^{1}H 7.26 *ppm*, ^{13}C 77.16 *ppm*; CD_3OD: ^{1}H 3.31 *ppm*, ^{13}C 49.00 *ppm*). Chemical shifts (δ) are expressed as parts-per-million (*ppm*) and coupling constants (*J*) as hertz (*Hz*).

HPLC analyses and purification were performed with a Waters Alliance e2695 Separations Module, equipped with a Waters 2998 UV/Vis Photodiode Array Detector and a Waters ACQUITY QDa Mass Detector for detecting the analytes and a XSelect CSH C18 OBD Prep Column (130Å, 5 µm, 10 mm X 150 mm, 1/pkg, Waters). Water with 0.1% formic acid (v/v) and acetonitrile with 0.1% formic acid (v/v) were used as mobile phases (named A and B, respectively) with the following gradient: concentration phase B: 5→25% from 0 to 4 min; 25% from 4 to 7 min; 25→100% from 7 to 9 min; 100→5% from 9 to 11 min; 5% from 11 to 12 min. The flow rate was of 3 mL min^{-1}. The purity of PAI compound was found to be ≥95%. High resolution mass spectroscopy measurements (ionization: NanoESI, positive ionization) were performed at the mass spectrometry core facility of the IRB (Barcelona, Spain) with a LTQ-FT Ultra (Thermo Scientific) for direct infusion (Automated Nanoelectrospray) of the sample. The NanoMate (AdvionBioSciences, Ithaca, NY, USA) aspirated the samples from a 384-well plate (protein Lobind) with disposable, conductive pipette tips, and infused the samples through the nanoESI Chip (which consists of 400 nozzles in a 20 x20 array) towards the mass spectrometer. Spray voltage was 1.70 kV and delivery pressure was 0.50 psi. Data are reported as mass-to-charge ratio (*m/z*) of the corresponding positively charged molecular ions.

1.2 Abbreviations

Solvents: AcOEt: ethyl acetate; DCM: dichloromethane; MeCN: acetonitrile; MeOH: methanol; EtOH: ethanol; THF: tetrahydrofuran; Et_2O: diethyl ether; iPr_2O: diisopropyl ether; DMSO: dimethylsulfoxide.

Analytical characterizations: NMR: d: doublet; dd: double doublet; ddd: double double doublet; dt: double triplet; m: multiplet; q: quartet; quin: quintet; s: singlet; t: triplet; m.p.: melting point; R_f: retention factor; r.t.: room temperature; RT: retention time.

1.3 Synthetic procedures

PAI and NAI were prepared by combining three different building blocks: (a) a photo-isomerizable spacer (**4**), (b) an allosteric fragment (**5** or **6**, respectively), and (c) an orthosteric Iperoxo-like moiety (**9**) (**Scheme S1**). The intermediate compounds **5**, **6** and **9** and Iperoxo were all prepared by following synthetic procedures reported in the literature.[1–3]

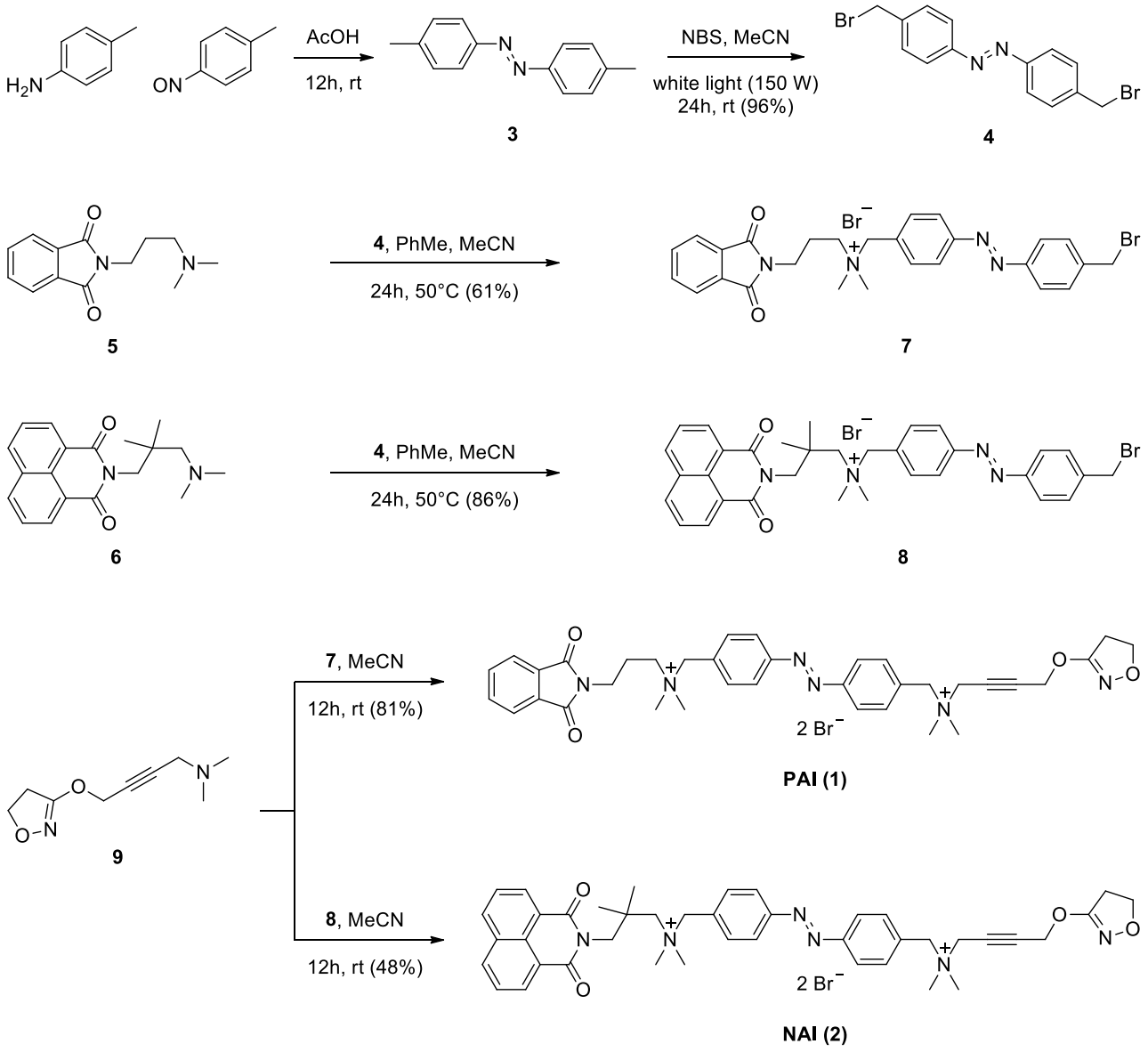

Scheme S1. Chemical synthesis of PAI and NAI.

4,4'-Bis(bromomethyl)azobenzene (4)

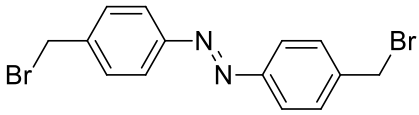

A solution 4,4′-dimethylazobenzene **3** (1.10 g, 5.23 mmol), prepared as reported by Velema et al.,[4] and *N*-bromosuccinimide (2.33 g, 13.08 mmol) in MeCN (200 mL) was stirred at room temperature under white light illumination (Dolan-Jenner Fiber-Lite Mi-150 Fiber Optic Illuminator, 150 W) for 24 hours. Then, the mixture was concentrated, and the obtained orange solid was filtered and washed several times with MeOH. The resulting solid was dried under vacuum to afford **4** as an orange solid (1.34 g, 96% yield).

M.p.: 228-230 ˚C

^{1}H NMR (400 MHz, $CDCl_3$): δ 7.90 (d, *J* = 8.4 Hz, 4H), 7.54 (d, *J* = 8.3 Hz, 4H), 4.56 (s, 4H). ^{13}C NMR (101 MHz, $CDCl_3$): δ 152.42, 140.93, 130.06, 123.51, 32.83.

_N_-(4-((4-(bromomethyl)phenyl)diazenyl)benzyl)-3-(1,3-dioxoisoindolin-2-yl)-_N_,_N_-dimethylpropan-1-aminium bromide (7)

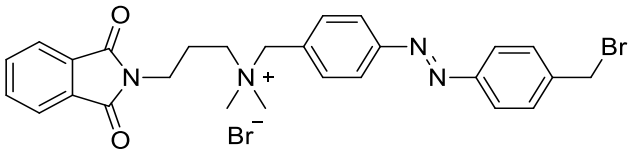

Azobenzene **4** (713 mg, 1.94 mmol) was completely dissolved in toluene (200 mL) at 70 °C, and the resulting solution was left under stirring at 50 °C. Then a solution of phthalimide **5** (50 mg, 0.22 mmol) in MeCN (50 mL) was slowly added dropwise. The reaction was left under stirring for 24 hours at 50 °C. Reaction progress was controlled by silica gel TLC to monitor the disappearance of the starting material **5** (eluent: DCM/MeOH, 95:5). At the end, the mixture was concentrated under reduced pressure and the resulting solid was washed several times with toluene in order to completely remove the excess azobenzene **4** and finally dried under reduced pressure to afford **7** as an orange solid (79 mg, 61%).

^{1}H NMR (400 MHz, CD_3OD): δ 7.98 – 7.89 (m, *J* = 8.8 Hz, 4H), 7.87 (dd, *J* = 5.5, 3.1 Hz, 2H), 7.80 (dd, *J* = 5.5, 3.1 Hz, 2H), 7.74 (d, *J* = 8.5 Hz, 2H), 7.64 (d, *J* = 8.4 Hz, 2H), 4.68 (s, 2H), 4.67 (s, 2H), 3.83 (t, *J* = 6.3 Hz, 2H), 3.48 – 3.40 (m, 2H), 3.14 (s, 6H), 2.37 – 2.25 (m, 2H). ^{13}C NMR (101 MHz, CD_3OD): δ 169.80, 154.98, 153.39, 143.78, 135.57, 135.15, 133.32, 131.29, 124.42, 124.35, 124.32, 68.52, 63.12, 50.81, 35.66, 33.00, 23.53.

LC-MS (QMS, $[M + H]^+$): calcd for $C_{27}H_{28}BrN_4O_2^+$, 519.14 and 521.14; found 519.3 and 521.2.

(_E_)-_N_-(4-((4-(bromomethyl)phenyl)diazenyl)benzyl)-3-(1,3-dioxo-1_H_-benzo[de]isoquinolin-2(3_H_)-yl)-_N_,_N_,2,2-tetramethylpropan-1-aminium bromide (8)

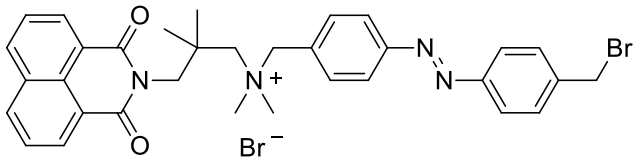

Azobenzene **4** (276 mg, 0.75 mmol) was completely dissolved in toluene (30 mL) at 70 °C, and the resulting solution was left under stirring at 50 °C. Then a solution of Naphthalimide **6** (25 mg, 0.08 mmol) in MeCN (20 mL) was slowly added dropwise. The reaction was left under stirring for 24 hours at 50 °C. Reaction progress was controlled by silica gel TLC to monitor the disappearance of the starting material **6** (eluent: DCM/MeOH, 95:5). At the end, the mixture was concentrated under reduced pressure and the resulting solid was washed several times with toluene in order to completely remove the excess azobenzene **4** and finally dried under reduced pressure to afford **8** as an orange solid (10 mg, 86%).

^{1}H NMR (400 MHz, CD_3OD): δ 8.56 (dd, *J* = 7.3, 1.1 Hz, 2H), 8.35 (dd, *J* = 8.5, 1.0 Hz, 2H), 7.95 (dd, *J* = 8.4, 3.2 Hz, 4H), 7.85 – 7.74 (m, 4H), 7.66 (d, *J* = 8.7 Hz, 2H), 4.73 (s, 2H), 4.68 (s, 2H), 4.30 (s, 2H), 3.55 (s, 2H), 3.32 (s, 6H), 1.41 (s, 6H). ^{13}C NMR (101 MHz, CD_3OD): δ 165.21, 153.44, 151.99, 142.34, 134.31, 134.23,

131.73, 131.23, 130.17, 129.89, 127.85, 126.81, 122.99, 122.84, 122.10, 72.62, 71.92, 51.06, 49.04, 39.16, 31.60, 25.31.

Phthalimide-Azo-Iperoxo, PAI (1)

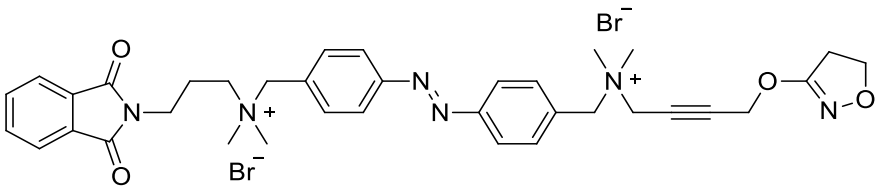

Compound **7** (50.4 mg, 0.08 mmol) and the isoxazoline **9** (30.6 mg, 0.17 mmol) were dissolved in MeCN (30 mL) and stirred at room temperature for 12 hours. Reaction progress was controlled by silica gel TLC to monitor the disappearance of the starting material **7** (eluent: DCM/MeOH, 9:1). PAI (**1**) was then isolated from the resulting solution by precipitation after adding a few drops of Et_2O to the reaction mixture, filtered, further washed with Et_2O (20 mL x 3), and dried under reduced pressure (53 mg, 81%).

^{1}H NMR (400 MHz, CD_3OD) δ 8.10 (d, *J* = 8.5 Hz, 2H), 8.02 (d, *J* = 8.5 Hz, 2H), 7.90 (dd, *J* = 5.6, 3.0 Hz, 2H), 7.85 (d, *J* = 8.5 Hz, 2H), 7.82 (dd, *J* = 5.6, 3.0 Hz, 2H), 7.75 (d, *J* = 8.5 Hz, 2H), 4.99 (t, *J* = 1.6 Hz, 2H), 4.74 (s, 2H), 4.64 (s, 2H), 4.41 (t, *J* = 9.6 Hz, 2H), 4.35 (t, *J* = 1.7 Hz, 2H), 3.84 (t, *J* = 6.3 Hz, 2H), 3.47 – 3.38 (m, 2H), 3.22 (s, 6H), 3.11 (s, 6H), 3.07 (t, *J* = 9.6 Hz, 2H), 2.37 – 2.24 (m, 2H).^{13}C NMR (101 MHz, CD_3OD) δ 169.79, 168.80, 163.40, 163.05, 162.71, 154.99, 154.83, 135.56, 135.28, 124.70, 124.54, 124.31, 88.78, 76.82, 71.22, 68.47, 67.39, 63.24, 58.29, 54.94, 50.90, 50.76, 35.65, 33.66, 23.51.

RT (HPLC-PDA) = 6.24 min (*cis* isomer), 6.67 min (*trans* isomer); purity≥ 95% (**Fig. S1.1**).

HR-MS (ESI, $[M + H]^+$): calcd for $C_{36}H_{42}N_6O_4^{2+}$, 311.16; found 311.1625 (**Fig. S1.2**).

Naphthalimide-Azo-Iperoxo, NAI (2)

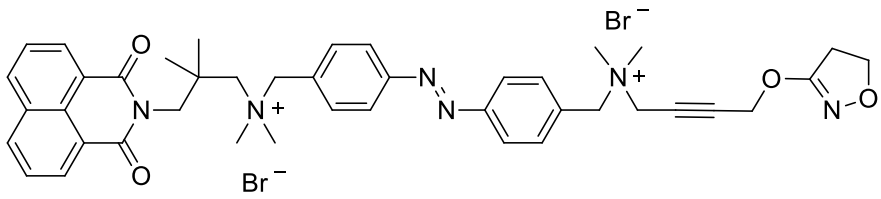

Compound **8** (10 mg, 0.015 mmol) and the isoxazoline **9** (4.03 mg, 0.022 mmol) were dissolved in MeCN (10 mL) and stirred at room temperature for 12 hours. Reaction progress was controlled by silica gel TLC to monitor the disappearance of the starting material **8** (eluent: DCM/MeOH, 9:1). NAI (**2**) was then isolated from the resulting solution by precipitation after adding a few drops of Et_2O to the reaction mixture, filtered, further washed with Et_2O (20 mL x 3), and dried under reduced pressure (6.10 mg, 48%).

^{1}H NMR (400 MHz, CD_3OD) δ 8.58 (dd, *J* = 7.3, 1.1 Hz, 2H), 8.37 (dd, *J* = 8.4, 1.1 Hz, 2H), 8.11 (d, *J* = 8.4 Hz, 2H), 8.01 (d, *J* = 8.4 Hz, 2H), 7.89 (d, *J* = 8.4 Hz, 2H), 7.86 – 7.77 (m, 4H), 4.99 (s, 2H), 4.79 (s, 2H), 4.76 (s, 2H), 4.48 – 4.38 (m, 4H), 4.31 (s, 2H), 3.58 (s, 2H), 3.33 (s, 6H), 3.25 (s, 6H), 3.07 (t, *J* = 9.6 Hz, 2H), 1.42 (s, 6H). ^{13}C NMR (101 MHz, CD_3OD) δ 168.82, 166.66, 155.00, 154.76, 135.79, 135.75, 135.41, 133.18,

132.66, 132.20, 131.85, 129.31, 128.26, 124.68, 124.46, 123.57, 88.70, 76.94, 74.28, 73.17, 71.23, 67.39, 58.35, 55.01, 52.53, 50.96, 50.48, 40.63, 33.69, 26.73.

HR-MS (ESI, $[M + H]^+$): calcd for $C_{36}H_{42}N_6O_4^{2+}$, 350.18; found 350.18630.

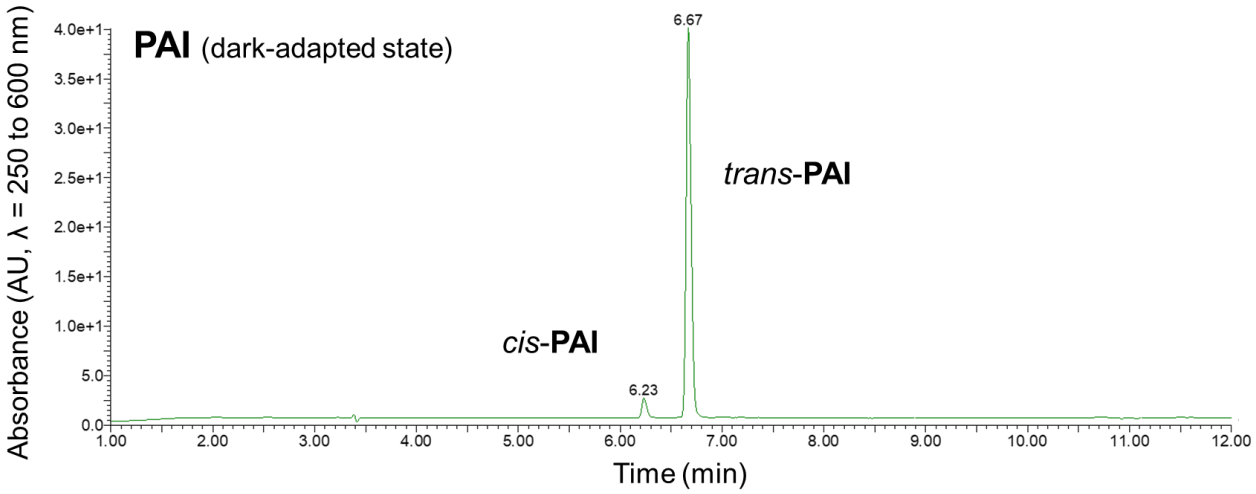

Fig. S1.1. HPLC chromatogram of PAI as obtained under benchtop conditions (PDA detector from 250 to 600 nm; compound purity ≥ 95%).

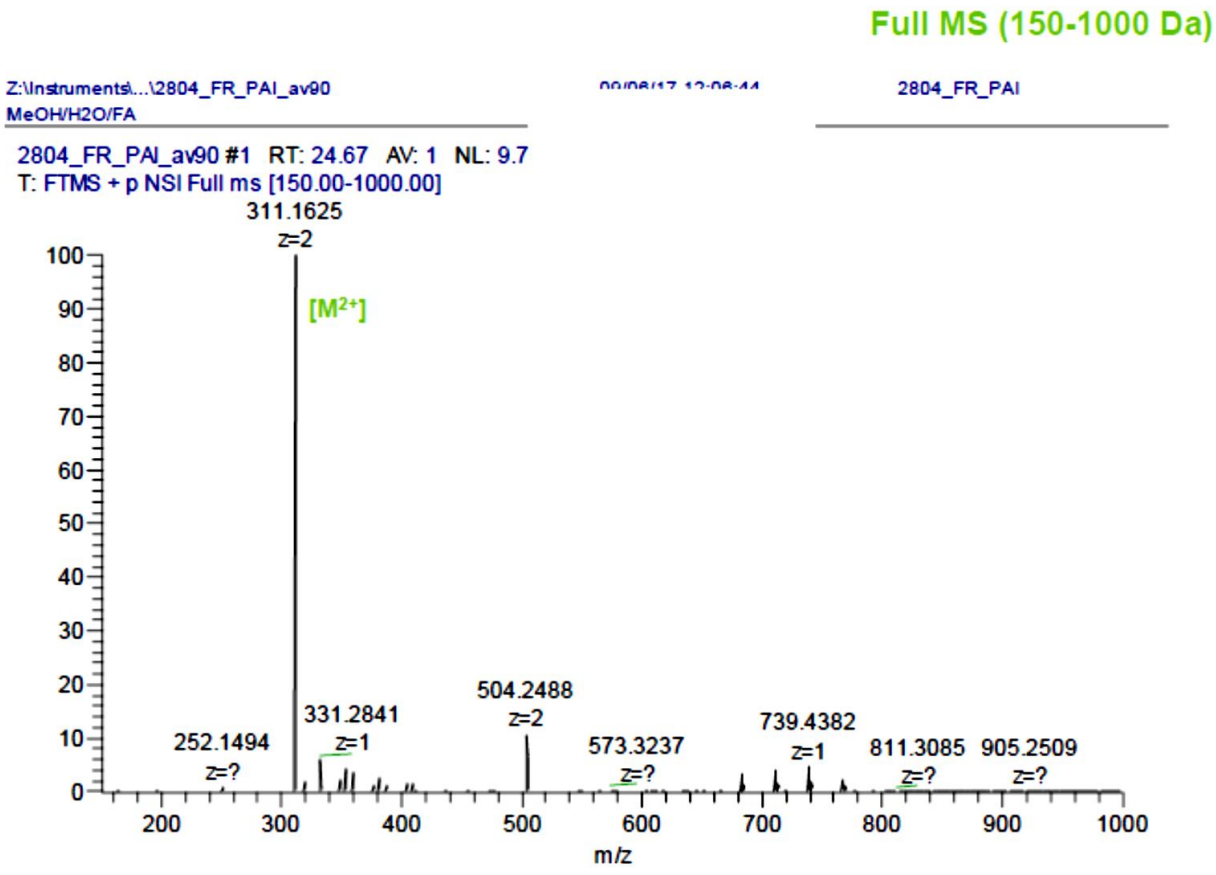

Fig. S1.2. Full high-resolution mass spectrum of **PAI** (positive ionization).

2. Photochemical characterization

An essential requirement for using PAI and NAI as light-regulated M2 mAChRs agonists is that they effectively respond to light, which means that they can be quickly photoisomerized (from *trans* to *cis* and vice versa) between two different conformations with a relatively high degree of photoconversion (*trans*/*cis* ratio). To this end, we characterized PAI and NAI by UV/Vis spectroscopy.

PAI revealed a clear photochromic behavior with the typical absorption bands of azobenzenes. Maximum absorption peaks in aqueous solution were observed at around 315 nm and 430 nm and are due to the π–π* and n–π* transitions, respectively, which allows for distinct photoswitching between the *trans* and *cis* isomers (**Fig. S2.1, panel A**). PAI can be effectively isomerized from *trans* to *cis* with ultraviolet light (365 nm), and back-isomerized from *cis* to *trans* with white or blue (460 nm) light. The process is reversible and can be repeated several times without any noticeable loss of photochromic behavior (**Fig. S2.1, panel B**).

Annoyingly, NAI resulted unusually refractory to photoisomerization than other azobenzene-containing compounds. We hypothesized that the absorption and emission properties of the naphthalimide moiety could interfere with the photoisomerization of the azobenzene unit (**Fig. S2.1, panels C and D**).

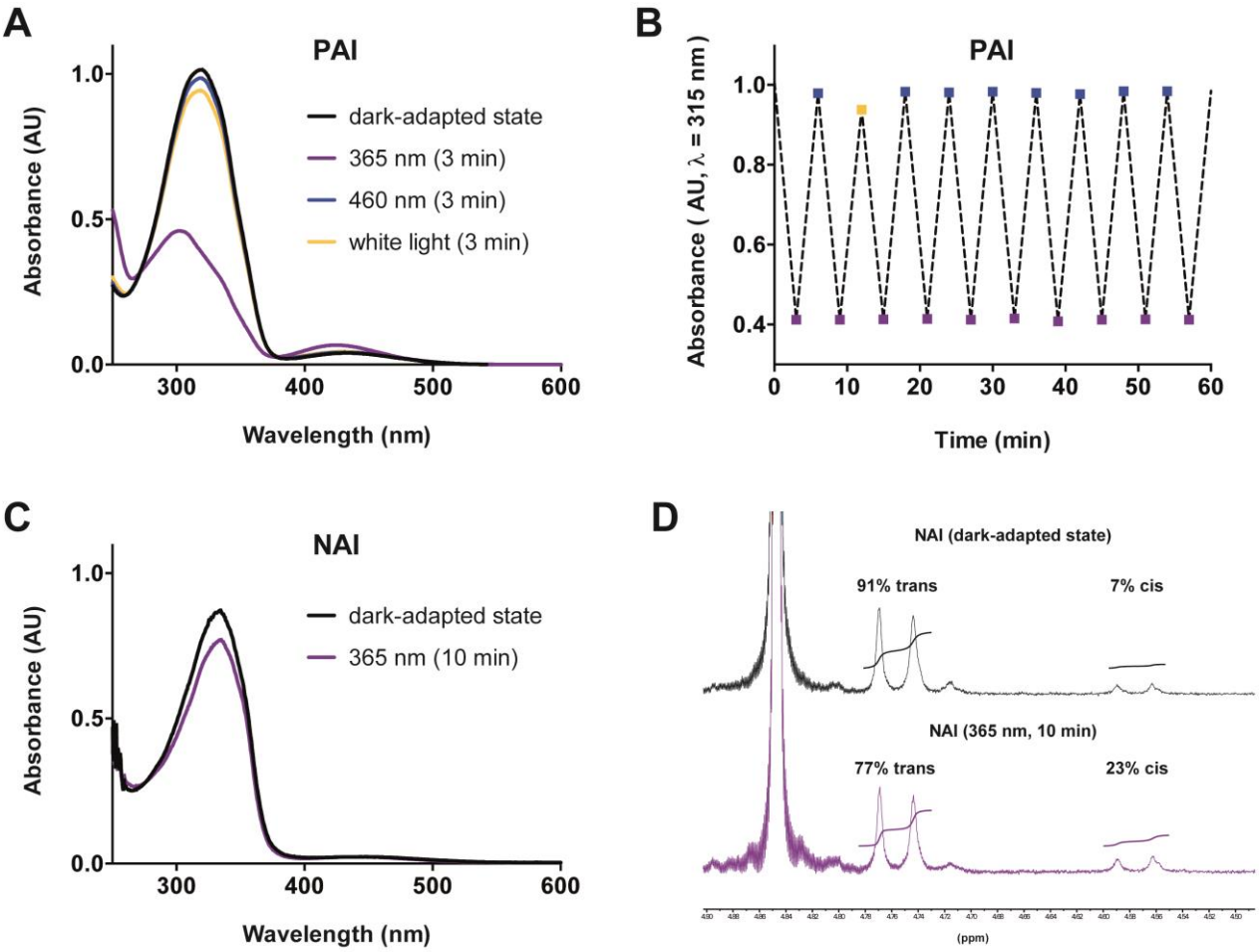

Fig. S2.1. Photochemical characterization of PAI and NAI. A) Absorption spectra of PAI in H_2O (30 µM). B) Reversibility and stability of the photochromic behavior of PAI over several cycles of isomerization. C) Absorption spectra of NAI in H_2O (30 µM). D) Quantification of NAI photostationary state by ^{1}H-NMR analysis (800 µM in CD_3OD), showing the ratio between the two isomers in the dark-adapted state and after illumination with 365 nm light (10 min).

We next quantified by ^{1}H-NMR and HPLC analysis the extent of photoisomerization for PAI (**Fig. S2.2**). The amount of the thermodynamically less stable *cis* isomer shifted from an initial value of 13% (as obtained under benchtop conditions) to 73% upon irradiation with 365 nm light for 10 minutes. Finally, we analyzed the thermal stability of the photostationary state (PSS) achieved after ultraviolet illumination. The PSS was relatively stable for at least 2 hours in aqueous solution at 37 °C in the dark. PAI could be rapidly reconverted to the *trans* state after illumination with white light. Such thermal stability allowed us to conveniently study the two different photostationary states of PAI in a relatively large timescale (**Fig. S2.3**).

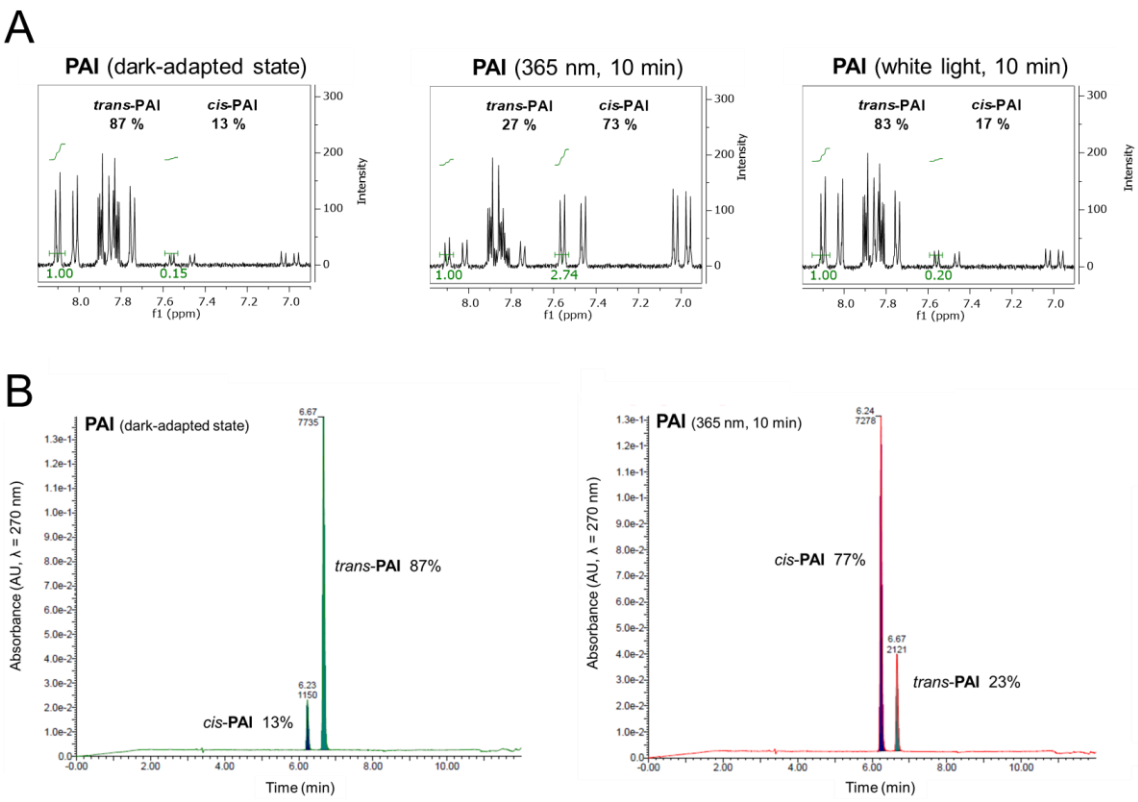

Fig. S2.2. Quantification of PAI photostationary state by ^{1}H-NMR (800 µM in CD_3OD, panel A) and HPLC (panel B) analysis, showing the ratio between the two isomers as obtained under benchtop conditions and after 10 minutes of irradiation with 365 nm light and white light.

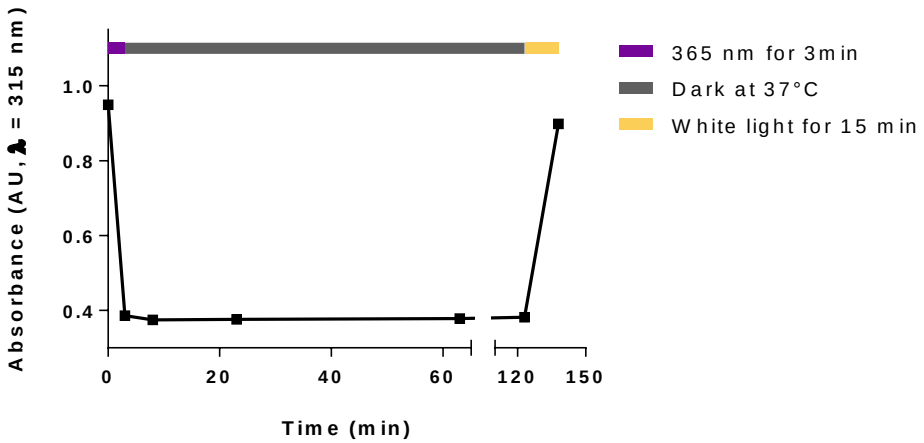

Fig. S2.3. Thermal stability of PAI. The photostationary state achieved after irradiation with 365 nm light in aqueous solution (30 µM) is stable for more than 2 hours at 37 °C in the dark. Irradiation with white light allows to rapidly regain a PSS in favor of the *trans* isomer.

3. NMR spectroscopy

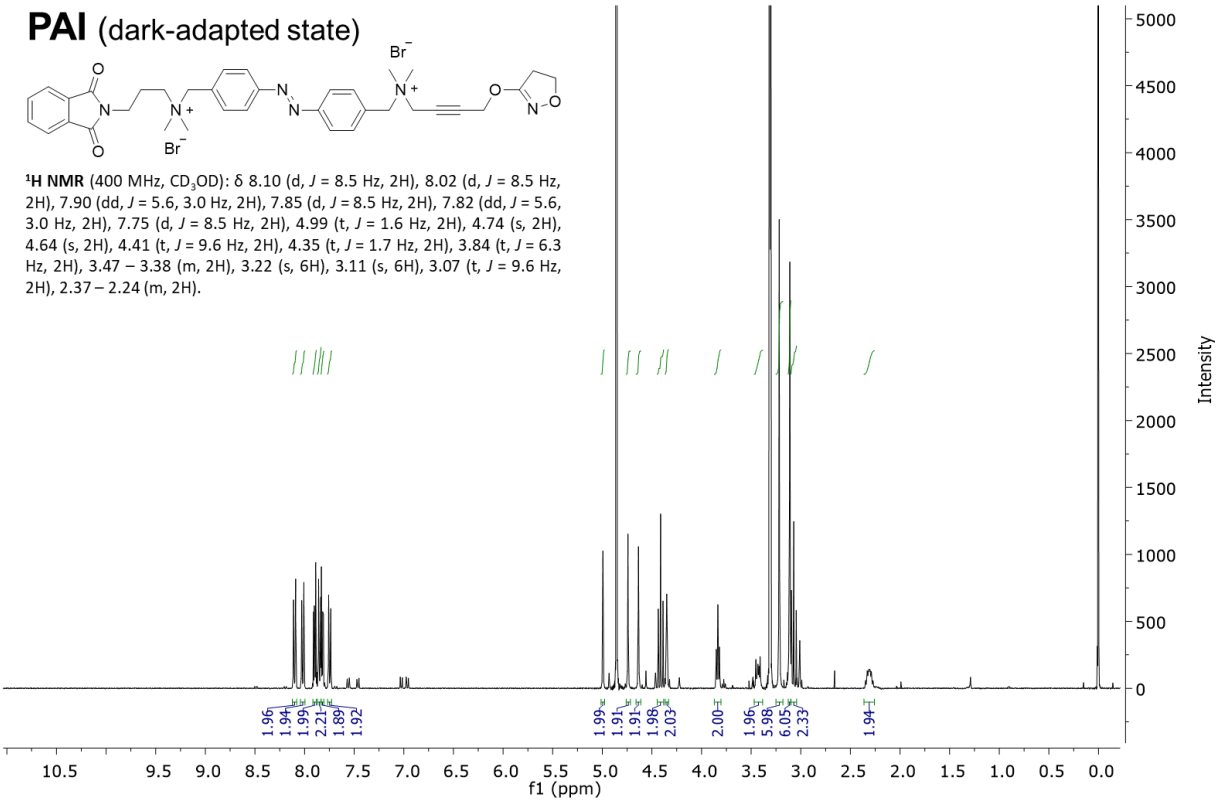

Fig. S3.1. ^{1}H-NMR of PAI as obtained under benchtop conditions.

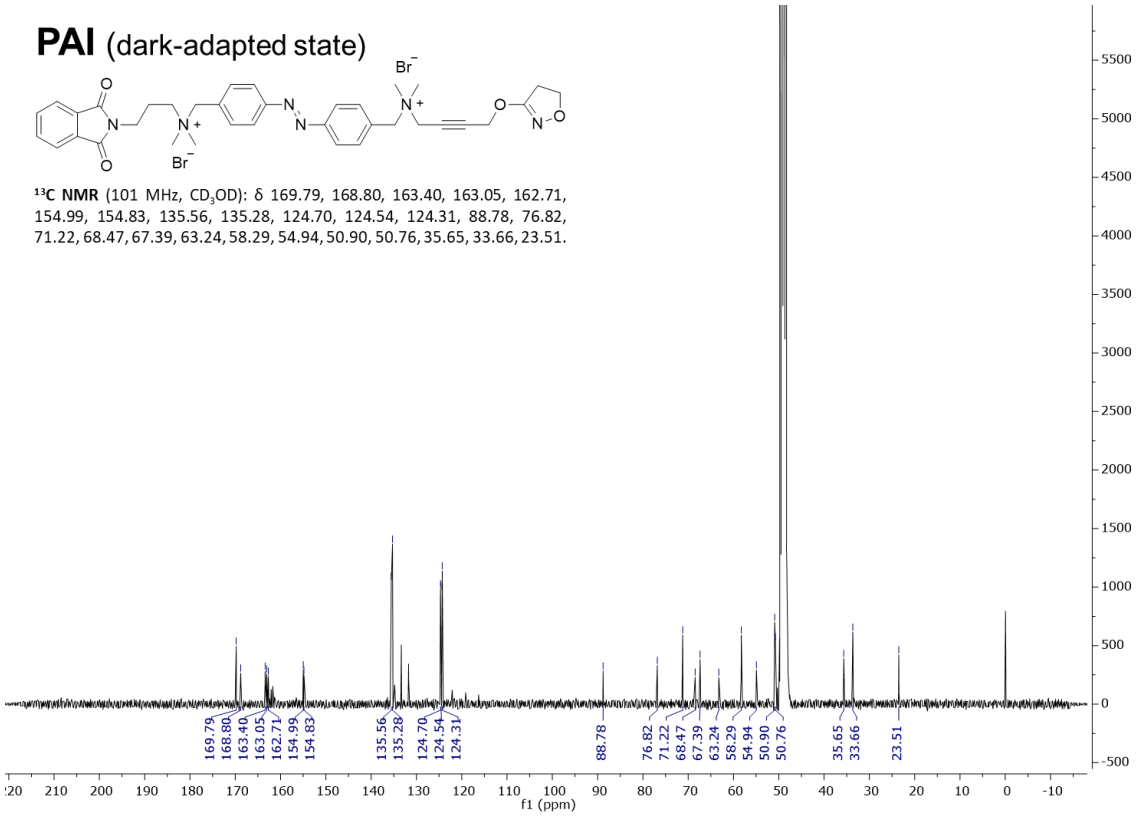

Fig. S3.2. ^{13}C-NMR of PAI as obtained under benchtop conditions.

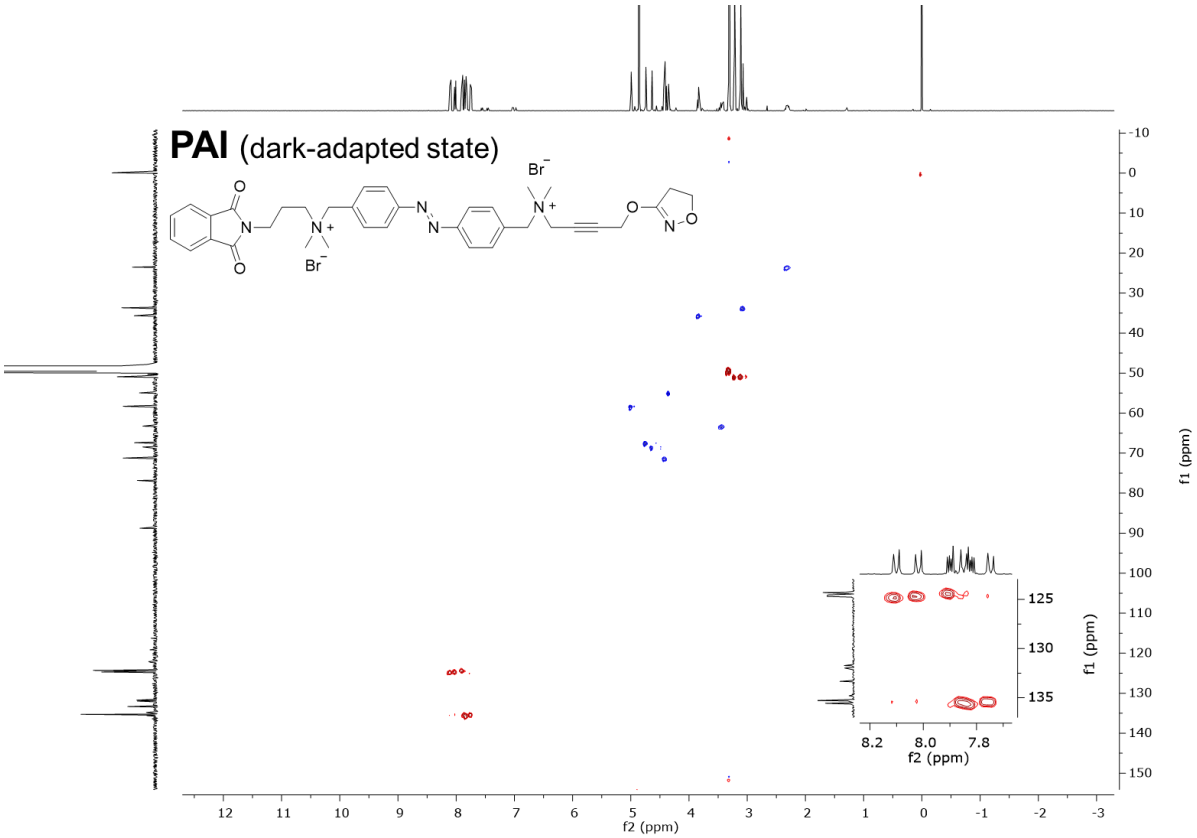

Fig. S3.3. gCOSY of PAI as obtained under benchtop conditions.

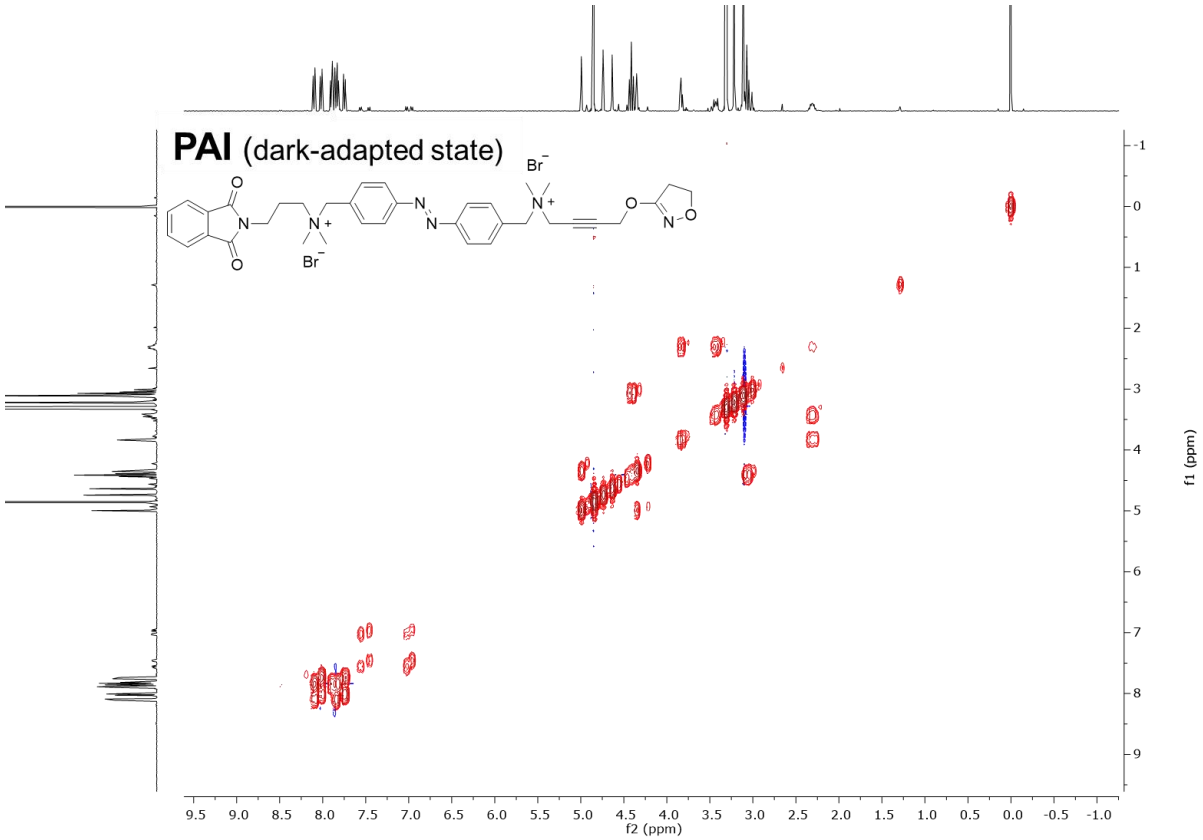

Fig. S3.4. HSQC of PAI as obtained under benchtop conditions.

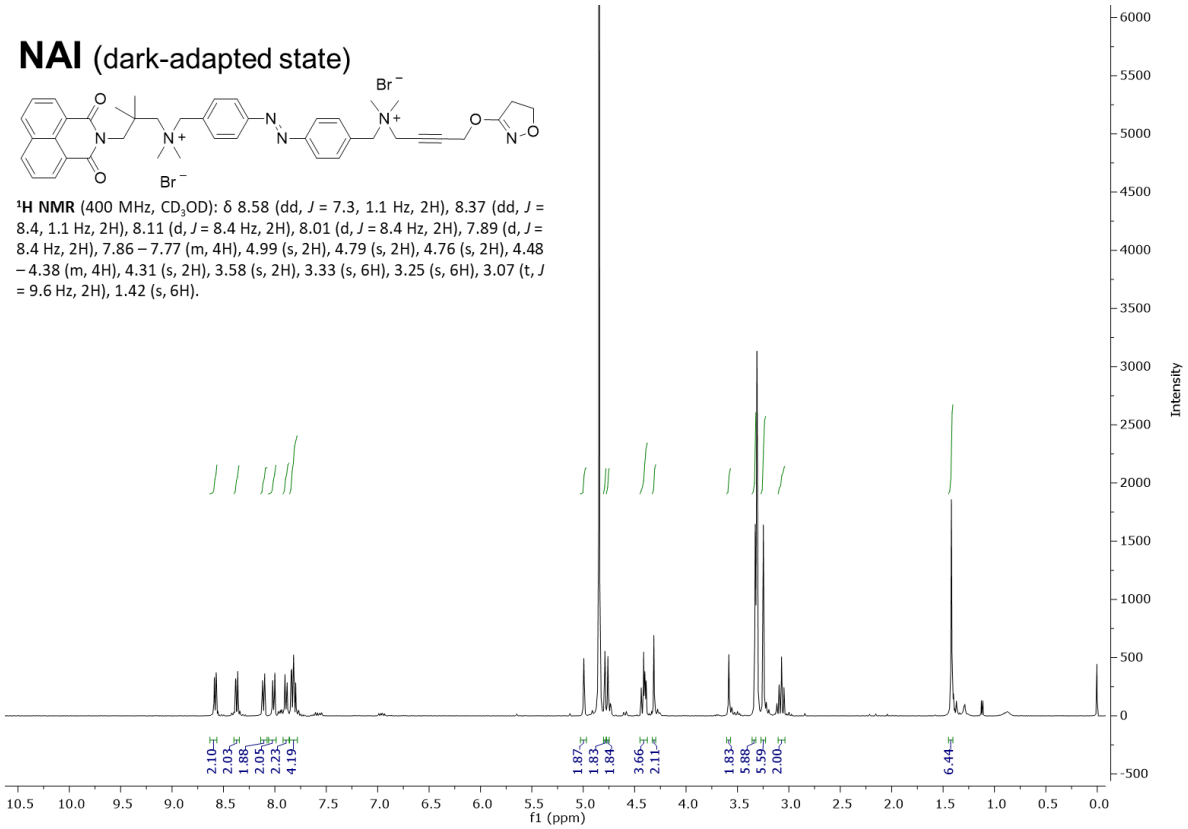

Fig. S3.5. ^{1}H-NMR of NAI as obtained under benchtop conditions.

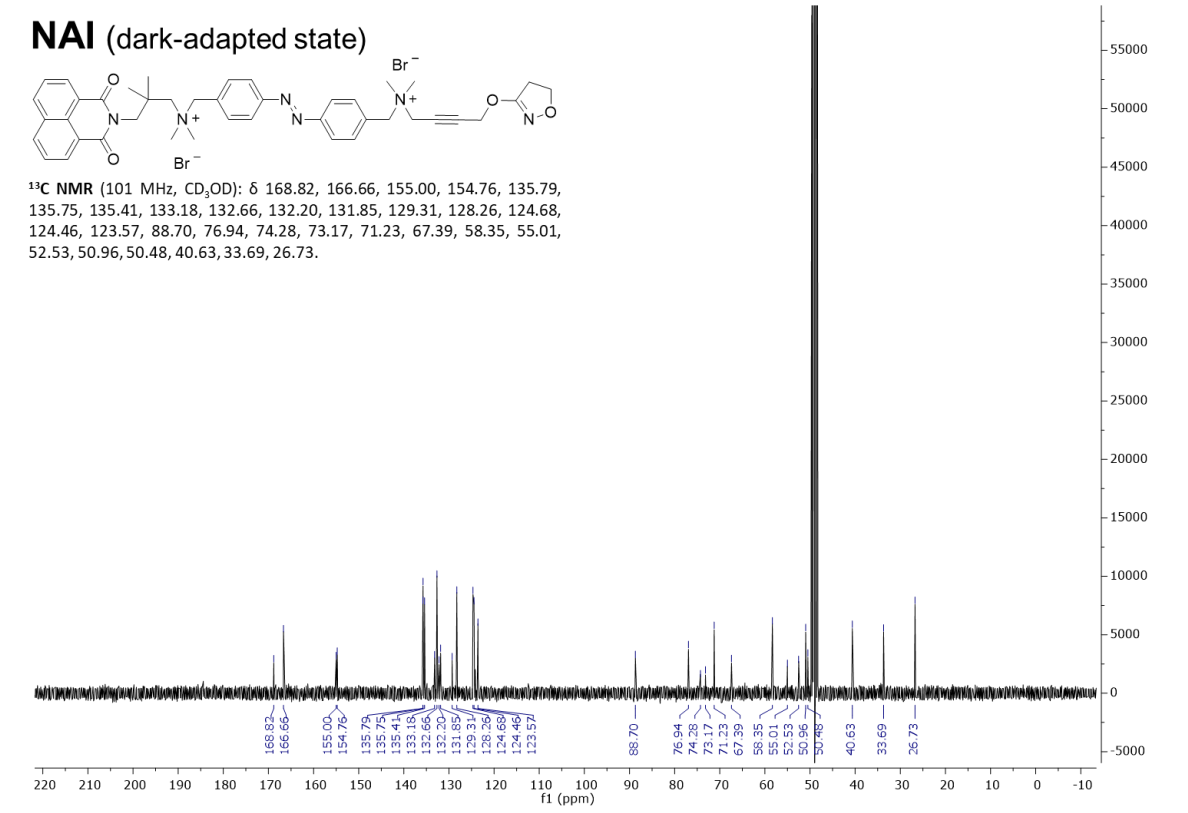

Fig. S3.6. ^{13}C-NMR of NAI as obtained under benchtop conditions.

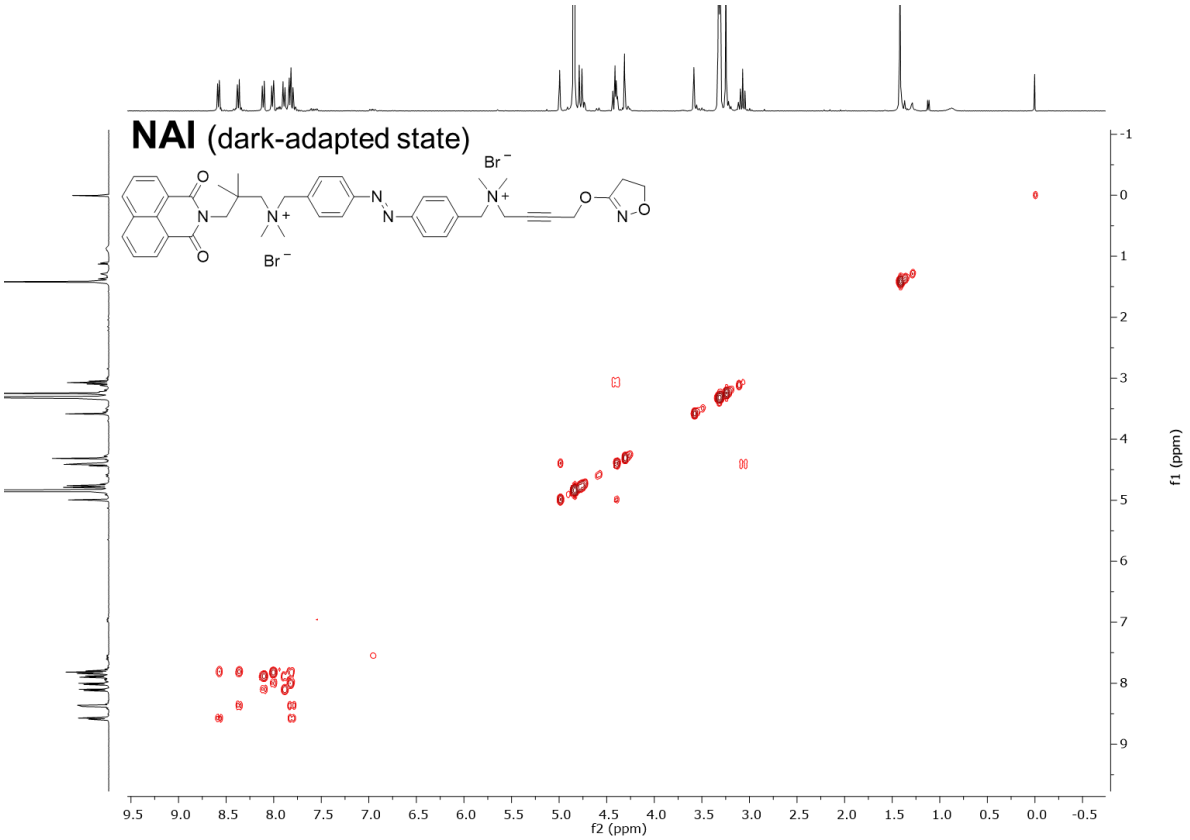

Fig. S3.7. gCOSY of NAI as obtained under benchtop conditions.

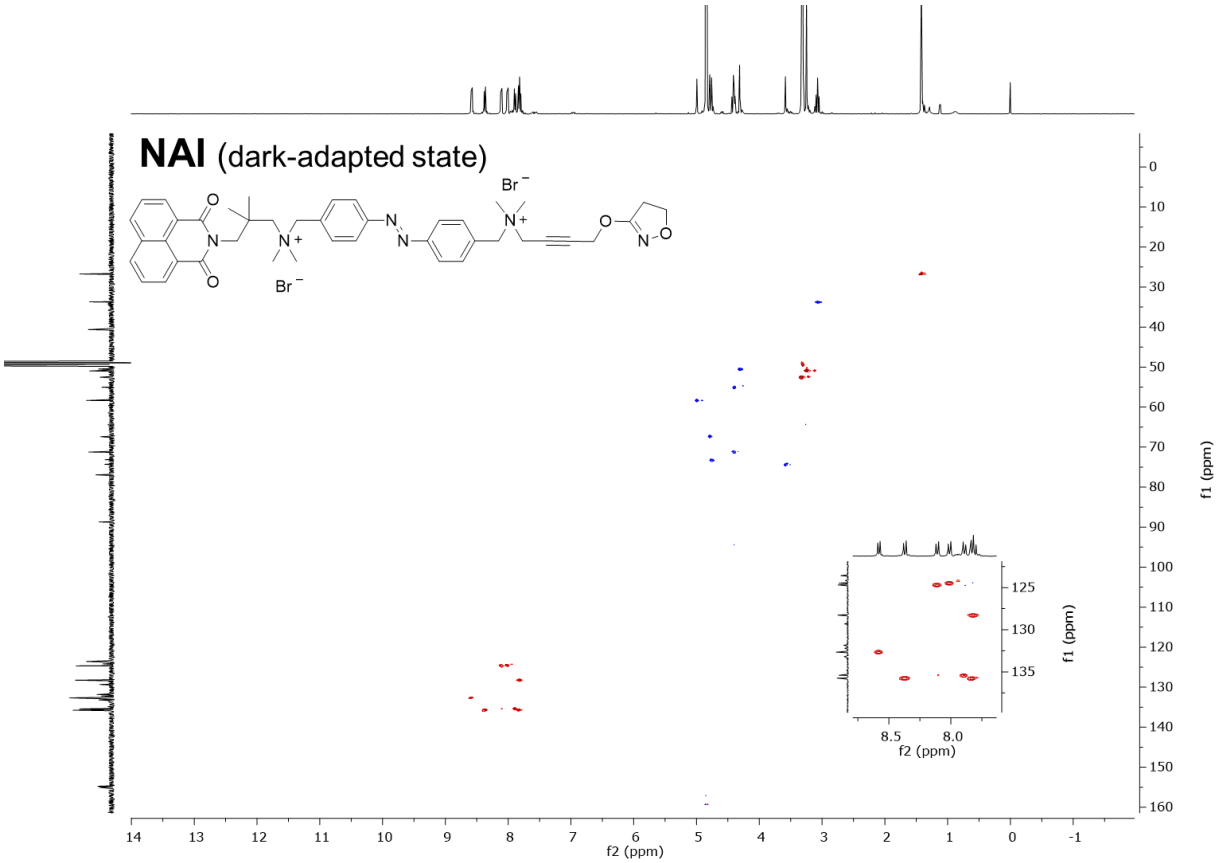

Fig. S3.8. HSQC of NAI as obtained under benchtop conditions.

4. *In vitro* calcium imaging experiments

4.1 Materials and methods

Since M2 mAChRs activate the G_i protein subfamily, we co-transfected a chimeric $G_{q/i}$-protein in order to couple M2 receptor activation to the phospholipase C pathway, thus inducing inositol 1,4,5-trisphosphate (IP3) production and subsequent intracellular calcium release from the endoplasmic reticulum.

Cell culture and transfection. HEK tsA201 cells were maintained at 37 °C in a humidified atmosphere with 5%CO_2 and grown in Dulbecco's Modified Eagle's Medium/Nutrient Mixture F-12 Ham (DMEM/F12 1:1, Life Technologies) medium, supplemented with 10% fetal bovine serum (FBS, Life Technologies) and antibiotics (1% penicillin/streptomycin, Sigma-Aldrich). Co-expression of human muscarinic acetylcholine receptor M2 (Addgene) and chimeric G_i/G_q protein (GqTOP) (ratio 1:1) was induced by plasmid transient transfection with X-tremeGENE 9 DNA Transfection Reagent (Roche Applied Science) following the manufacturer's instructions.[5] The day after transfection, cells were harvested with accutase (Sigma-Aldrich) and seeded onto 16-mm glass coverslips (Fisher Scientific) pretreated with collagen (Sigma-Aldrich) to allow cell adhesion. Preconfluent cultures were used for experiments between 48 h and 72 h after transfection.

In vitro single-cell calcium imaging. The bath solution used for single cell intracellular calcium recordings contained: 140 mM NaCl, 5.4 mM KCl, 1 mM $MgCl_2$, 10 mM HEPES, 10 mM glucose and 2 mM $CaCl_2$, and was adjusted to pH 7.4 with NaOH. Before each experiment, cells were mounted on the recording chamber (Open Diamond Bath Imaging Chamber for Round Coverslips from Warner Instruments) and loaded with the calcium indicator Oregon Green BAPTA-1, AM (OGB-1AM) (Life Technologies) for 30 min at 37 °C and 5% CO_2, at a final concentration of 10 μM in Ca^{2+}-free bath solution. Cells were rinsed with fresh solution, and the recording chamber was filled with 1 mL recording solution. Calcium imaging was performed on an IX71 inverted microscope (Olympus) with a XLUMPLFLN 20XW x20/1-NA water immersion objective (Olympus).

OGB-1 AM was excited during 8 ms at 488 nm using a Polychrome V monochromic light source (Till Photonics) equipped with a Xenon Short Arc lamp (Ushio) and a 505 nm dichroic beam splitter (Chroma Technology). Emission at 526 nm was filtered by a D535/40nm emission filter (Chroma Technology) and finally collected by a C9100-13 EM-CCD camera (Hamamatsu).

Images under 1P-illumination were acquired at room temperature with an imaging interval of 4 seconds with the SmartLux software (HEKA), and the imaging analysis was done with FIJI (ImageJ).

Images under 2P-illumination were acquired at room temperature with an inverted laser-scanning confocal microscope (TCS SP5, Leica Microsystems) equipped with a HCX PL APO 40×/1.25-0.75-NA oil objective for imaging cultured cells, and a HC PL APO 20×/.0.7-NA CS air objective (Leica Microsystems). The imaging interval was of 4 seconds. Acquired image sequences were stored in the Leica image format and stacks for offline analysis with FIJI (ImageJ).

Drug application and photoswitching assays. Addition of agonists was carried out by carefully pipetting 50 μL of the initial 200 pM solution of the compound directly into the accessory pool of the recording chamber for a final dilution of approximately 1:20.

Iperoxo, a previously described muscarinic selective superagonist,[2] was used as a positive control to stimulate mAChRs in HEK tsA201 cells (30 pM).

Photostimulation under 1P-excitation during recordings was done by illumination of the entire focused field using the Polychrome V connected to a personal computer, and shutter and wavelength were controlled using Patchmaster software (HEKA). Light intervals lasted a total of 5 minutes for all the HEK cell experiments, with flashes of blue (460 nm, 3.5-seconds duration) and UV (365 nm, 3.5-seconds duration) light. The light power measured with a Newport 1916-C light meter placed after the objective was16.48 $W \cdot m^{-2}$ for 488 nm, 4.94 $W \cdot m^{-2}$ for 365 nm, and 15.92 $W \cdot m^{-2}$ for 460 nm.

2P-excitation experiments were performed in the Advanced Digital Microscopy Core Facility of IRB Barcelona with a confocal multiphoton microscope equipped with a pulsed broadband Ti:Sapphire laser (Mai Tai, Spectra-

Physics, Santa-Clara, CA-USA) which can be tuned from 710-990 nm (80 MHz repetition rate, 80 fs pulse, light power 2.8 mW μm^{-2} at 720–840 nm).

4.2 Control experiments

In order to assess the significance of PAI (photo)responses in M2 mAChR expressing cells (**Fig. 3**), further control experiments were performed in transfected cells in absence of PAI (**Fig. S4.1**). No responses were observed under illumination at 365 nm and 460 nm which excludes any response artifacts due to light stimuli alone.

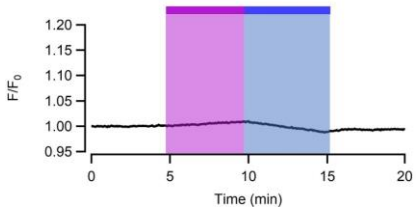

Fig. S4.1. Real time calcium imaging traces from HEK cells incubated with 10μM of OGB-1AM for 30 min. The diagrams show **A**) the average trace of cells expressing M2-GqTOP in response to illumination at 365 nm (purple bar) and 460 nm (blue bar) (n = 34 ± SEM); **B**) the average trace of cells expressing M2-GqTOP in response to 2P-excitation at 840 nm (red bar) (n = 29 ± SEM);

4.3 Receptor activation efficacy

Direct *cis*-PAI isomer application at 10 pM induce a response 50% lower than direct application of *trans*-PAI isomer. Application of the *cis* isomer at 30 pM induced a response 10-fold lower compared to the *trans* isomer response at the same concentration (**Fig. S4.2**). Moreover, residual responses upon application of the *cis* isomer can be attributed to the incomplete photoisomerization of the *trans*-isomer (*trans/cis* = 23:77 after 10 min at 365 nm).

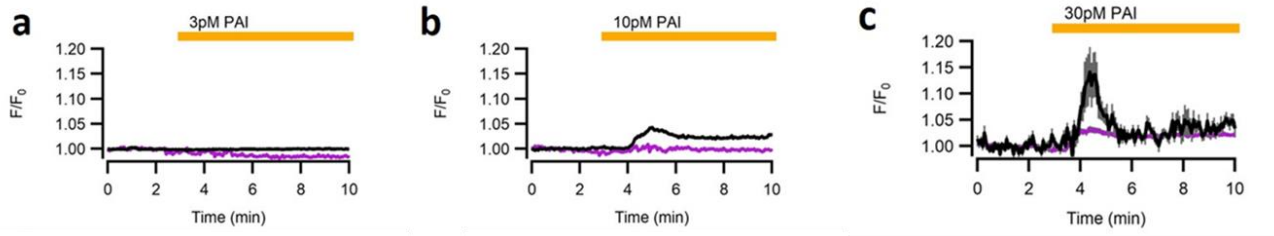

Fig. S4.2. Real time calcium imaging traces from HEK cells expressing M2-GqTOP incubated with OGB-1AM (10 μM for 30 min). A) Average trace of cell response induced by the direct application of 3 pM PAI (yellow bar) in its *trans* isoform (black line; n = 167) or its *cis* isoform (purple line; n = 150). B) Average trace of cell response induced by the direct application of 10 pM PAI in its *trans* isoform (black line; n = 296) or its *cis* isoform (purple line; n = 150). C) Average trace of cell response to 30 pM PAI in its *trans* isoform (black line; n = 8) or its *cis* isoform (purple line; n = 230). Gray shadow in the recording represents ± SEM.

4.3 Receptor subtype selectivity

Receptor subtype-selectivity of PAI (M2 against M1 mAChRs) has been studied by comparing amplitude of calcium signal response of cells expressing M2-GqTOP or M1 mAChR in presence of *trans*-PAI (10 pM). Human M1 mAChR (Addgene) was transfected as described in the *Materials and methods* section of the main text. M2 mAChR transfected cells gave a significantly higher response than M1 mAChR expressing cells (8% for M1 against 33% for M2). Data were normalized over the maximum response obtained with the nonselective orthosteric superagonist IPX at 30 pM. (*t*-test of two samples assuming equal variances $p = 0.00158$).

5. Molecular docking simulations

5.1 Materials and methods

Molecular docking simulations were performed using the crystal structure of the human M2 muscarinic acetylcholine receptor retrieved from the Protein Data Bank (PDB code: 4MQT, chain A).[6] To allow the docking of the dualsteric ligands into the active M2 AChR structure, the so called "tyrosine lid"[7,8] was remodeled using rotamer libraries (UCSF Chimera)[9] of the tyrosine residues involved (Tyr-104, Tyr-403, Tyr-426). The protein pdb file was then prepared for docking by removing co-crystallized ligands, non-complexed ions and water molecules, and finally applying the Dock Prep tool available in the free software package UCSF Chimera. This involved the addition of hydrogens and assigning partial charges (AMBER ff14SB method). The structures of *trans*- and *cis*-PAI were built with standard bond length and angles using ChemDraw and then energy minimized with Chem3D by the MM2 method. The minimized compounds were further prepared for docking studies with UCSF Chimera by adding hydrogens and assigning partial charges (AMBER ff14SB method). The necessary pdbqt files of ligands and receptor were prepared using AutoDock 4.2 software. The docking studies were carried out using the standard docking protocol applied for AutoDock Vina in PyRx 0.8 virtual screening software. Autodock Vina has been reported to be an effective tool capable of quickly and accurately predicting bound conformations and binding energies of ligands with macromolecular targets.[10,11] A grid box of size 10.08 × 27.44 × 28.96 Å, with x, y and z coordinates of –2.98, –11.92 and –12.00, respectively, was fixed to cover the entire allosteric and orthosteric binding sites and accommodate the ligands to move freely. Docking studies were performed using an exhaustiveness value of 8 while all other parameters were maintained as defaults. All rotatable bonds within the ligands were allowed to rotate freely, and the receptor was considered rigid. The docking simulations were repeated three times for each ligand. The obtained poses were then ranked based on the predicted affinity docking scores (kcal/mol) and the best pose for each experiment was selected. The results were then analyzed using UCSF Chimera.

5.2 Results and discussion

We used molecular docking simulations in an attempt to rationalize the photoswitchable efficacy of PAI. Both isomers of the ligand were docked into their putative allosteric and orthosteric binding sites of the human M2 muscarinic acetylcholine receptor in its active conformation (PDB code: 4MQT, chain A). As previously reported,[7] molecular docking of dualsteric ligands into the M2 mAChR required remodeling of the tyrosine lid (formed by Tyr-104, Tyr-403 and Tyr-426) which separates the orthosteric binding site from the allosteric binding site in the active conformation of the protein. To open this lid and put the two binding sites in communication, we selected different allowed conformers of each side chains while keeping all the other residues in their original position. Therefore, the only differences between the crystal structure and the obtained active-like receptor model were the side chain conformations of Tyr-104, Tyr-403 and Tyr-426. *Trans*-PAI and *cis*-PAI were docked at this receptor model using a standard docking protocol with AutoDock Vina in the PyRx 0.8 software with a suitable grid box. We ran three simulations for each ligand and selected the best pose obtained in each experiment based on the predicted binding affinity scores (kcal/mol). Best poses were superimposed into the M2 receptor model in the presence of the reference agonist Iperoxo (in its receptor-bound conformation) and analyzed using UCSF Chimera. The results of our *in silico* studies are presented in **Table S1** and **Fig. S5.1**.

In Iperoxo, key binding elements for agonist activity are (a) the positively charged nitrogen, which interacts with Asp-103 and displays *π*-cation interactions with Tyr-104, Tyr-403 and Tyr-426, (b) the triple bond, which exhibits hydrophobic contacts with Tyr-104, Trp-155 and Trp-400, and additionally (c) the oxygen of the 4,5-dihydroisoxazole moiety, which forms a hydrogen bond with Asn-404.[8] Our simulations revealed a dualsteric binding topography of PAI in both configurations. The Iperoxo moiety of *trans*-PAI binds to the orthosteric binding site, with an orientation close to that observed for Iperoxo in the receptor-bound crystal structure and the key elements for agonist activity lying in proximity of those of the reference agonist, whereas the phthalimide moiety protrudes toward extracellular domains, likely engaging residues of the common allosteric

binding site (**Fig. S5.1a**). In agreement with our results, *trans*-PAI could therefore bind to the M2 mAChR in a dualsteric pose capable of inducing receptor activation. In contrast, *cis*-PAI appeared to bind preferentially in a flipped orientation, with the phthalimide group pointing out towards the orthosteric binding pocket and the 4,5-dihydroisoxazole moiety positioned in the allosteric binding site. Such a binding mode is not likely to form an active ligand-receptor complex and may justify the difference observed in terms of agonist efficacy between the two photo-isomers (**Fig. S5.1b**).

	***trans*-PAI (best pose)**	***cis*-PAI (best pose)**
experiment number	***binding affinity (kcal/mol)***	
1	-11.6	-12.0
2	-11.6	-11.8
3	-11.3	-11.6

Table S1. Binding affinity scores of the best poses for each of the docking studies performed with *trans*- and *cis*-PAI.

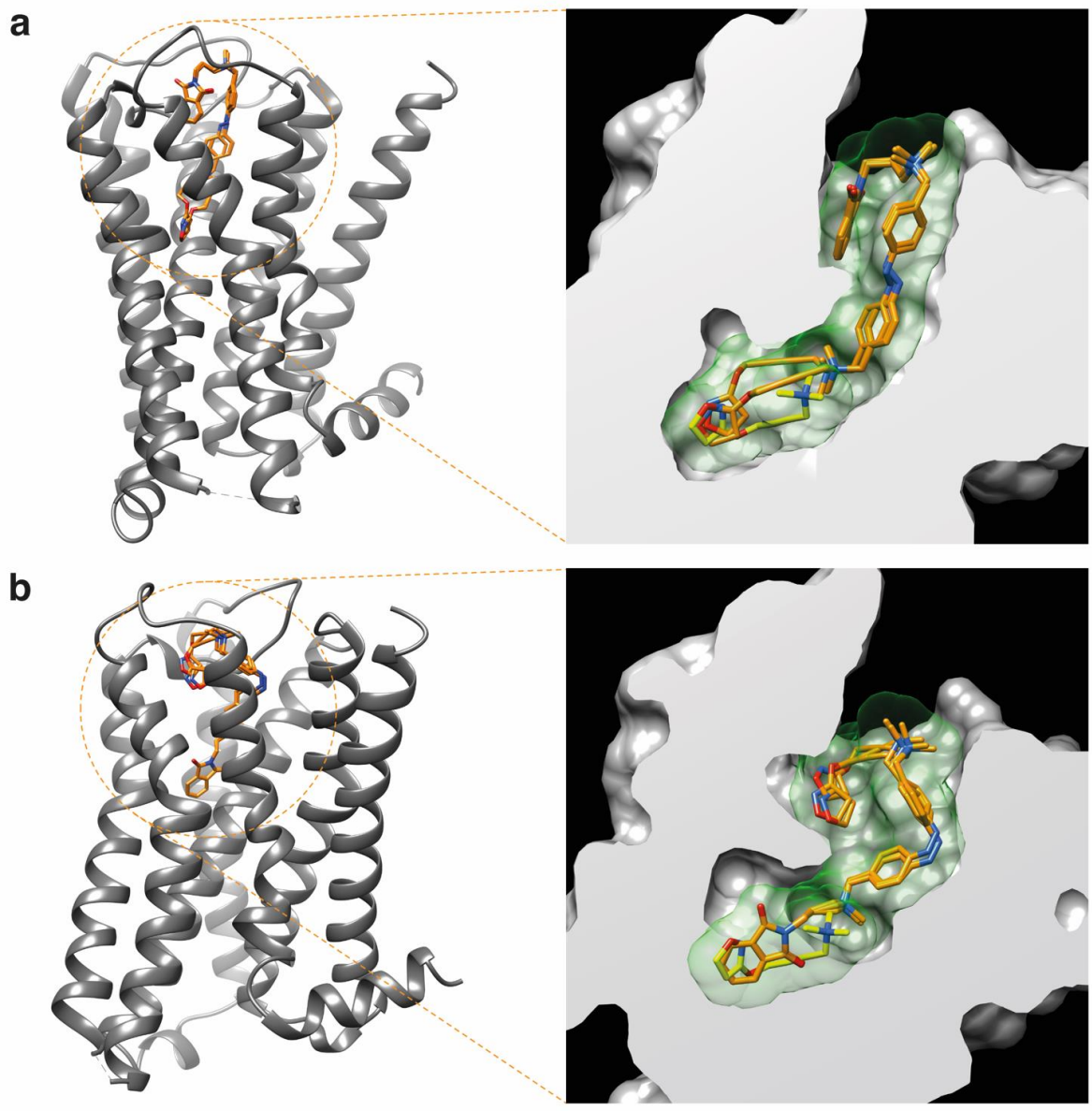

Fig. S5.1 Hypothetical binding mode of *trans*-PAI and *cis*-PAI to a M2 mAChR model in its active state. Panels (*a*) and (*b*) show a full view (left side, ribbon-style representation) and a zoomed view (right side, hydrophobicity surface representation with sectioning) of the simulated ligand-receptor complexes. The reference orthosteric agonist Iperoxo, in yellow, appears in its receptor-bound conformation. *Trans* and *cis*-PAI are represented in orange. Nitrogen and oxygen atoms of the ligands are colored in blue and red, respectively. Our simulations revealed a dualsteric binding topography of PAI for both configurations, but, while the *trans* isomer seems to bind preferentially in an Iperoxo-like binding pose (Panel *a*), which is likely able to trigger receptor activation, the *cis* isomer shows preference for a flipped orientation (Panel *b*), which might be not compatible with the formation of active ligand-receptor complexes.

6. *In vivo* experiments in rats

6.1 Materials and methods

In vivo effects of PAI in both configurations (*trans* and *cis*) were further tested in male Wistar rats (400-500 g) under inhaled anesthesia (isoflurane 1.5%) and maintained at 37±0.3 °C with a homothermic pad (Kent Scientific, Torrington, CT, US). All animals had a continuous electrocardiogram (ECG) obtained (lead II) and recorded for later offline analyses (PowerLab and LabChart v.8.1.2, ADInstruments, Colorado Springs, CO, US). Analyses were performed in a blinded manner.

Nine rats were randomly assigned to receive cumulative doses of either predominantly *trans*- ("trans" group, n = 5) or *cis*-isomer ("cis" group n = 4) PAI. A single stock solution was used for all experiments, and dilutions were prepared just prior to each experiment. In the "*cis*" group, a vial containing 1 mL of PAI solution was irradiated with UV-light lamp (365 nm) in a custom-made closed chamber for 5 minutes, and thereafter administered intraperitoneally in dark conditions. Two animals (one for each "*cis*" and "*trans*" groups) were initially used to delimitate the effective dose range, which was found to be in the range of 100 nM/kg – 100 µM/kg (results not shown). Subsequently, the following PAI doses were intraperitoneally administered at 7-minute intervals in the remaining rats: 100 nM/kg; 300 nM/kg; 1 µM/kg; 3 µM/kg; 10 µM/kg; 30 µM/kg; 100 µM/kg.

The heart rate (beats·min^{-1}) and the PR interval (ms) were measured offline to assess the parasympathetic effect of both PAI isomers (LabChart v.8.1.2, ADInstruments, Colorado Springs, CO, US). A one-minute recording (from minute 5'30" to minute 6'30" after each dose administration) of stable ECG was analyzed. Heart rate and the PR interval were automatically determined, manually reviewed for accuracy, and modified if needed. Second degree Wenckebach atrio-ventricular block and subsequent complete block occurred in one rat receiving the 30 µM/kg dose and one rat receiving the 100 µM/kg dose, and were excluded from PR interval measurements. Results are shown as difference to the baseline value (Δ).

In order to test that parasympathetic activity was driving heart rate and PR-interval changes, and to assess its reversibility, atropine (two 1 mg doses separated by 5-7 minutes) was administered to one rat per group. A representative profile of a full experiment is shown in **Fig. S6.1**.

Data analysis and statistics. In vivo data is shown in boxplots. Because some rats died after the administration of high doses of the active isomer *trans*-PAI, a maximum effect asymptotic value was not reached and a formal dose-response curve could not be built. Therefore, analyses were carried out with a two-way ANOVA in which two main factors (Isomer, Dose) and their interaction (Isomer x Dose) were included. In the case of a significant interaction, pairwise comparisons (Isomer effect at each Dose) were performed with the LSD test.

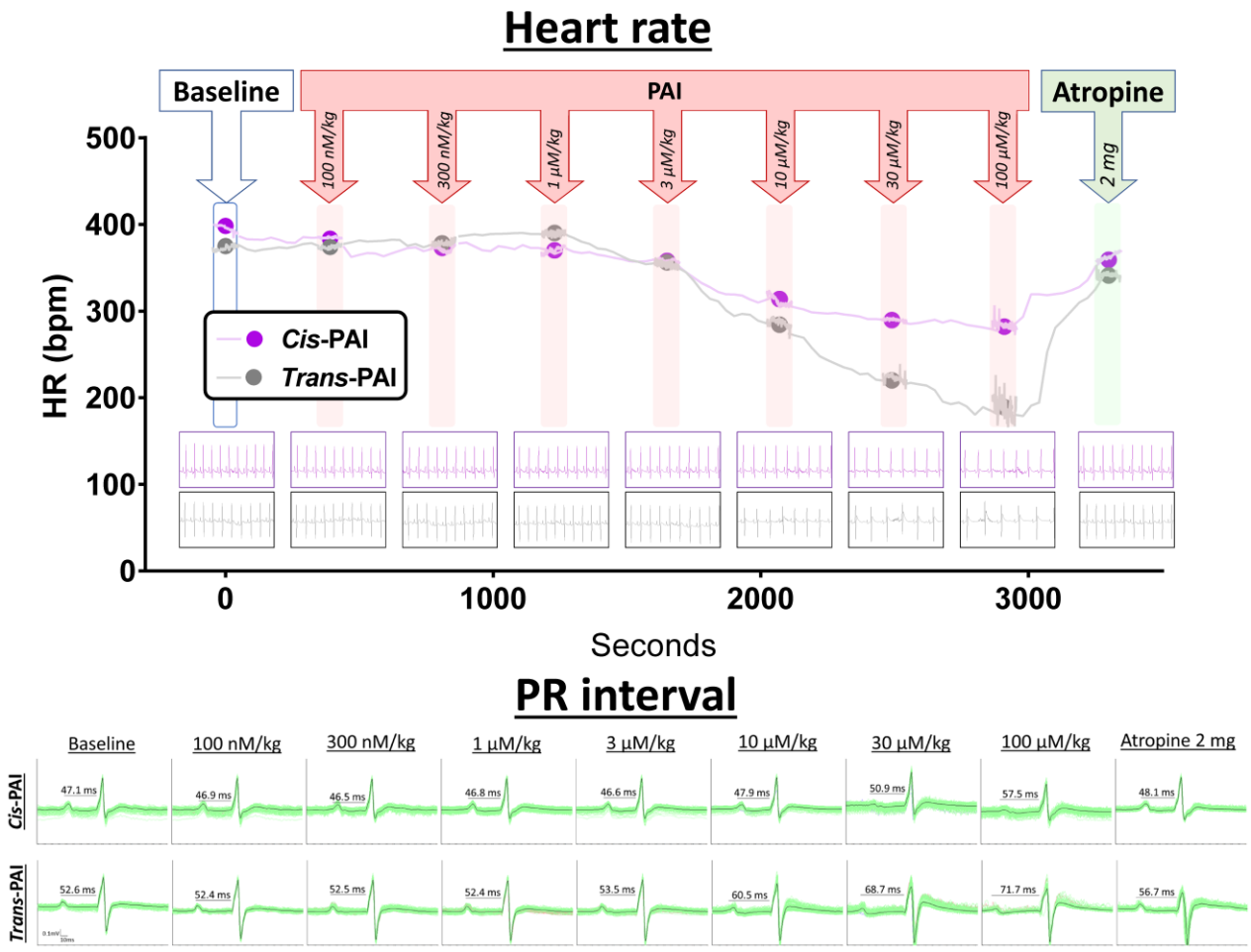

Fig. S6.1. Representative profile of the heart rate (upper panel) and the PR interval (lower panel) in two rats receiving increasing doses of PAI (*trans* or *cis* form), and atropine. Heart rate is averaged every second in shadowed areas in the upper panel; in between doses, heart rate is averaged every 30 seconds.

7. *In vivo* experiments in *Xenopus tropicalis* tadpoles

7.1 Materials and methods

African clawed frogs constitute an excellent animal model for behavioral, genetic and electrophysiological studies,[12,13] and a powerful tool for drug discovery and preclinical animal testing.[14] In addition, they are especially suitable for heart monitoring since tadpoles are transparent until stages 48-50[15] and, in contrast to fish, their three-chamber heart is an excellent model for studying the human cardiovascular system.[16,17]

Animal housing. Xenopus tropicalis embryos (Nasco) were obtained by natural mating and maintained till 3-4 days post fertilization (dpf) in 0.1X Marc's modified Ringer's (MMR) solution in agarose coated Petri dishes (10-15 cm diameter) in a dark incubator (24 °C). Animals were transferred to tanks containing Xenopus water, which was prepared by adding 8 g of instant ocean salt (Instant Ocean) to 20 L of distilled water. Conductivity and pH were 700 µS and 7.4-7.5, respectively. Tadpoles were kept at a density of 30-50 animals L-1, at 24 °C and fed daily with spirulina. All procedures complied with the standards of the ethical commission of the University of Barcelona. *Xenopus tropicalis* tadpoles (developmental stages 44-48 according to Nieuwkoop and Faber)[15] were paralyzed in 0.23 mM of Pancuronium dibromide solution (PCD) (Merck, Cat no. P1918) for 10 minutes and placed into a 48-well plate (Nunc™Microwell™) with 200µL of 0.1X solution of MMR-$CaCl_2$ (referred as BS from now on). PCD was preferred to tricaine because of its higher cardiac tolerability and non-UV dependent effects.[17]

Cardiac activity measurements. Video recordings of tadpole hearts were performed using a Nikon Eclipse TS100 microscope equipped with an OptixCam Summit Series OCS-D3K2-5 camera, which substantially improved the resolution of the previously reported setup.[18] In order to prevent unintended *cis*-to-*trans* isomerisation of photoswitchable compounds, the microscope top-down light pathway was dimmed with a red plastic filter, which could be placed or removed during experimentation. Video recordings were acquired using the ToupView software, enhancing visual contrast to improve cardiac imaging and video streams were converted to the AVI format. Recordings were briefly interrupted during compound addition and changes of illumination conditions. Video information and data analysis were extracted and executed with custom scripts based on ImageJ[19] for AVI files analysis and subsequently converted to the TXT format for R software analysis.[20]

The illumination protocol established for control and treatment video recordings applied the following procedure: one minute dimmed red light (650 nm, 34.0 $W \cdot m^{-2}$), three minutes under UV (365nm, 2.3 $W \cdot m^{-2}$) due to the required exposure time for a complete *trans*-to-*cis* isomerisation, two minutes dimmed red light and one minute under visible light (455 nm, 169.8 $W \cdot m^{-2}$) for *cis*-to-*trans* back isomerisation.

Tadpoles (n = 4) were firstly paralyzed with PCD as previously described, placed in the BS and video recorded under the established protocol of illumination in the absence of PAI to monitor the effect of the light on cardiac activity and verify control conditions. Afterwards, animals were placed into a 10 µM PAI solution and underwent the same protocol of illumination to observe the light-dependent effects of the drug.

Data analysis and statistics. Heart beating movies were converted to a linear signal by selecting a region of interest displaying large periodic variations corresponding to heart movements, and calculating the corresponding grey scale level as a function of time (**Fig. 5a-d**). The cardiac rate (beats$\cdot s^{-1}$) was calculated from this linear signal from the number of maxima every 15 s (red plots in **Fig. 5e**). To statistically compare between different illumination periods and drug conditions, the cardiac rate was calculated from the last 30 s of every period. The stability of cardiac rhythm in each period was quantified with a unit-less variability score as the number of video frames between heartbeats. High scores correspond to longer periods with asynchronic or arrested cardiac activity. Perfectly steady rate in the absence of PAI yields a variability score of 8 (**Fig. S7.2**).

Statistical analyses were carried out with a two-way repeated measures ANOVA with uncorrected Fisher's Least Significant Differences (LSD) test in which two main factors (heart beats per second, 10 µM of PAI) and their interaction (heart beats per second x 10 µM of PAI) were included (**Fig. 5f**).

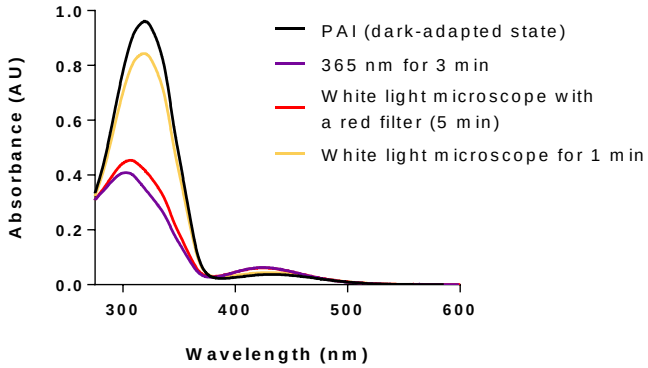

Fig. S7.1. Validation of the photochromic behavior of PAI under the illumination conditions used for our *in vivo* experiments in *X. tropicalis* tadpoles. PAI could be effectively isomerized to *cis* under illumination with 365 nm light (external source) and back-isomerized to *trans* using unfiltered microscope white light (100% intensity), whereas the *cis*-enriched photostationary state could be satisfactorily maintained when the microscope light was filtered with a common red polycarbonate filter.

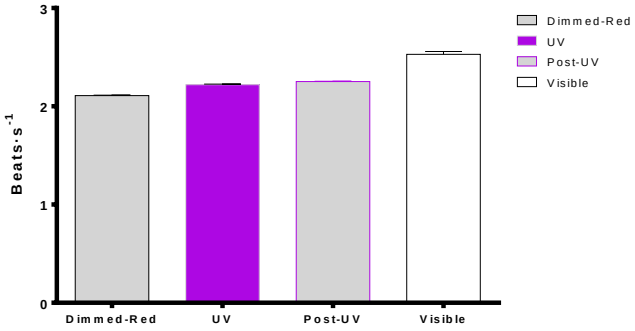

Fig. S7.2. Cardiac activity (beats per second) recorded under different conditions of illumination in absence of PAI (control experiment). Error bars represent SEM (n = 4).

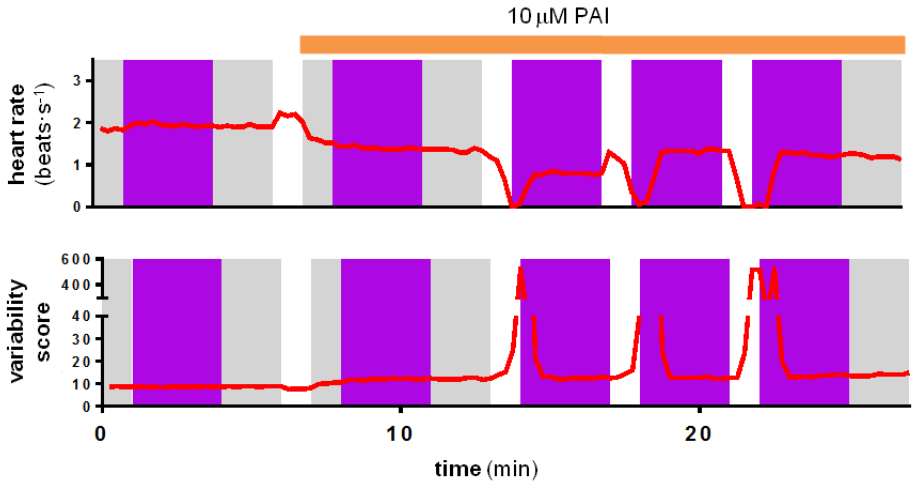

Fig. S7.3. Example trace of cardiac rate from one animal in **Fig. 4** (top) and corresponding variability score calculated as the number of video frames between heartbeats (averaged every 15 s). Although the first exposure to 10 µM *trans*-PAI did not immediately reduce the heart rate of this animal, subsequent cycles of UV/white light in the presence of PAI reversibly switched the heartbeat on and off. Reduced heart rate was associated with longer periods displaying unstable, asynchronic cardiac activity and thus a higher variability score.

8. Additional references

(1) Dallanoce, C.; Conti, P.; De Amici, M.; De Micheli, C.; Barocelli, E.; Chiavarini, M.; Ballabeni, V.; Bertoni, S.; Impicciatore, M. Synthesis and Functional Characterization of Novel Derivatives Related to Oxotremorine and Oxotremorine-M. *Bioorg. Med. Chem.* **1999**, *7* (8), 1539–1547.

(2) Kloeckner, J.; Schmitz, J.; Holzgrabe, U. Convergent, Short Synthesis of the Muscarinic Superagonist Iperoxo. *Tetrahedron Lett.* **2010**, *51* (27), 3470–3472.

(3) Disingrini, T.; Muth, M.; Dallanoce, C.; Barocelli, E.; Bertoni, S.; Kellershohn, K.; Mohr, K.; De Amici, M.; Holzgrabe, U. Design, Synthesis, and Action of Oxotremorine-Related Hybrid-Type Allosteric Modulators of Muscarinic Acetylcholine Receptors. *J. Med. Chem.* **2006**, *49* (1), 366–372.

(4) Velema, W. A.; van der Toorn, M.; Szymanski, W.; Feringa, B. L. Design, Synthesis, and Inhibitory Activity of Potent, Photoswitchable Mast Cell Activation Inhibitors. *J. Med. Chem.* **2013**, *56* (11), 4456–4464.

(5) Gomeza, J.; Mary, S.; Brabet, I.; Parmentier, M. L.; Restituito, S.; Bockaert, J.; Pin, J. P. Coupling of Metabotropic Glutamate Receptors 2 and 4 to G Alpha 15, G Alpha 16, and Chimeric G Alpha Q/i Proteins: Characterization of New Antagonists. *Mol. Pharmacol.* **1996**, *50* (4).

(6) Kruse, A. C.; Ring, A. M.; Manglik, A.; Hu, J.; Hu, K.; Eitel, K.; Hübner, H.; Pardon, E.; Valant, C.; Sexton, P. M.; et al. Activation and Allosteric Modulation of a Muscarinic Acetylcholine Receptor. *Nature* **2013**, *504* (7478), 101–106.

(7) Antony, J.; Kellershohn, K.; Mohr-Andrä, M.; Kebig, A.; Prilla, S.; Muth, M.; Heller, E.; Disingrini, T.; Dallanoce, C.; Bertoni, S.; et al. Dualsteric GPCR Targeting: A Novel Route to Binding and Signaling Pathway Selectivity. *FASEB J.* **2009**, *23* (2), 442–450.

(8) Bock, A.; Bermudez, M.; Krebs, F.; Matera, C.; Chirinda, B.; Sydow, D.; Dallanoce, C.; Holzgrabe, U.; De Amici, M.; Lohse, M. J.; et al. Ligand Binding Ensembles Determine Graded Agonist Efficacies at a G Protein-Coupled Receptor. *J. Biol. Chem.* **2016**, *291* (31), 16375–16389.

(9) Pettersen, E. F.; Goddard, T. D.; Huang, C. C.; Couch, G. S.; Greenblatt, D. M.; Meng, E. C.; Ferrin, T. E. UCSF Chimera--A Visualization System for Exploratory Research and Analysis. *J. Comput. Chem.* **2004**, *25* (13), 1605–1612.

(10) Morris, G. M.; Huey, R.; Lindstrom, W.; Sanner, M. F.; Belew, R. K.; Goodsell, D. S.; Olson, A. J. AutoDock4 and AutoDockTools4: Automated Docking with Selective Receptor Flexibility. *J. Comput. Chem.* **2009**, *30* (16), 2785–2791.

(11) Dallakyan, S.; Olson, A. J. Small-Molecule Library Screening by Docking with PyRx. In *Methods in molecular biology (Clifton, N.J.)*; 2015; Vol. 1263, pp 243–250.

(12) Grainger, R. M. Xenopus Protocols. **2012**, *917*, 1–11.

(13) Burggren, W. W.; Warburton, S. Amphibians as Animal Models for Laboratory Research in Physiology. *ILAR J.* **2007**, *48* (3), 260–269.

(14) Schmitt, S. M.; Gull, M.; Brändli, A. W. Engineering Xenopus Embryos for Phenotypic Drug Discovery Screening. *Adv. Drug Deliv. Rev.* **2014**, *69–70*, 225–246.

(15) Nieuwkoop P., F. J. *Normal Table of Xenopus Laevis (Daudin): A Systematical & Chronological Survey of the Development from the Fertilized Egg till the End of Metamorphosis*; 1994.

(16) Boppart, S. A.; Tearney, G. J.; Bouma, B. E.; Southern, J. F.; Brezinski, M. E.; Fujimoto, J. G. Noninvasive Assessment of the Developing Xenopus Cardiovascular System Using Optical Coherence Tomography. *Proc. Natl .Acad. Sci. USA* **1997**, *94* (9), 4256–4261.

(17) Bartlett, H. L.; Scholz, T. D.; Lamb, F. S.; Weeks, D. L. Characterization of Embryonic Cardiac Pacemaker and Atrioventricular Conduction Physiology in Xenopus Laevis Using Noninvasive Imaging. *Am. J. Physiol. Heart Circ. Physiol.* **2004**, *286* (6), H2035-41.

(18) Eckelt, K.; Masanas, H.; Llobet, A.; Gorostiza, P. Automated High-Throughput Measurement of Body Movements and Cardiac Activity of Xenopus Tropicalis Tadpoles. *J. Biol. Methods* **2014**, *1* (2), 9.

(19) Schindelin, J.; Arganda-Carreras, I.; Frise, E.; Kaynig, V.; Longair, M.; Pietzsch, T.; Preibisch, S.; Rueden, C.; Saalfeld, S.; Schmid, B.; et al. Fiji: An Open-Source Platform for Biological-Image Analysis. *Nature Methods*. 2012, pp 676–682.

(20) R-Core Team. A Language and Environment for Statistical Computing. 2016.